Original research Article

In situ synthesis of PANI/CuO nanocomposites for non-enzymatic electrochemical glucose sensing

Gul Rahman*, Mustifuz Ur Rahman, Zainab Najaf

*Institute of Chemical Sciences, University of Peshawar, Peshawar 25120, Pakistan. E-mail: gul_rahman47@uop.edu.p
pk*

ABSTRACT

We report the in situ synthesis of polyaniline/copper oxide (PANI/CuO) nanocomposites and their characterization as electrocatalyst for non-enzymatic electrochemical glucose detection. Copper oxide (CuO) nanoparticles were prepared by wet chemical precipitation method followed by thermal treatment while the composites of PANI and CuO were synthesized by in situ chemical polymerization of aniline with definite amount of CuO. X-ray diffraction (XRD) results revealed that the composites are predominantly amorphous. The composite formation was confirmed by fourier transform infrared (FTIR) and UV-Vis spectroscopy analysis. The surface morphology was greatly altered with the amount of CuO in composite structure. PANI/CuO nanocomposites were coated on copper substrate to investigate their electrocatalytic activity for glucose sensing. PANI/CuO with 10 wt. % CuO exhibited good response towards electrochemical glucose oxidation.

Keywords: Polyaniline; Copper Oxide; Nanocomposites; Electrocatalyst; Glucose Sensing

ARTICLE INFO

COPYRIGHT

1. Introduction

Diabetes mellitus, a chronic metabolic disorder, resulting from glucose concentrations lower or higher than the normal range (4.4–6.6 mM)[1]. The increasing number of diabetic patients has compelled scientists to search for fast and stable technologies to detect blood glucose level. The development of rapid, simple, effective, highly selective, biocompatible, easily portable, environment friendly and inexpensive glucose sensors are extremely desirable in several fields, including pharmaceutics, clinical diagnostics and food industry[2]. Enzyme-based electrodes using glucose oxidase (Gox), due to their selectivity and high sensitivity have been extensively used to design various amperometric biosensors for the detection of glucose[3]. Besides their potential applications in biosensing, enzyme-modified electrodes have a number of drawbacks, including inadequate thermal stability, high cost of enzymes, acute functioning environments and complex procedure of immobilization. Moreover, the environmental conditions such as humidity, pH value, ionic detergents, temperature and toxic chemicals can easily affect the catalytic activity of Gox[4,5].

Researchers are nowadays taking interest to develop simple enzyme-free glucose sensors with desirable properties of sensitivity, selectivity, environment friendly, stability, using simple organic and inorganic precursors. For this purpose, electrodes modified with pure metals[6,7], alloys[8,9], metal/metal oxide[10,11] and composites of conduc-

ting polymers with other materials[12,13] have been developed. However, the high cost of rare metals, poor sensitivity, narrow linear range and reduced selectivity to glucose, possibly due to the surface etching or poisoning during the electrochemical process that have limited their potential applications in biosensors[14]. Hence, the development of a highly sensitive, cheap and free of interference sensor for non-enzymatic monitoring of glucose is still critically required. The organic conducting and non-conducting polymers due to their facile synthesis and low cost are nowadays used for the preparation of a number of nonenzymatic biosensors. The polymer provides a matrix for immobilization of enzyme or inorganic catalyst having a three dimensional arrangement and have been used for the detection of carbohydrates in alkaline and neutral medium[15]. The conclusion derived from these studies showed that polymer based modified electrodes are advantageous due to ease of fabrication, wider linear response range, having good stability and low detection limits.

Recently, PANI has drawn considerable interest due to their unique conducting properties and has been largely applied in biosensing owing to its distinctive and controllable electrochemical characteristics[16], its environmental[17], thermal[18] and electrochemical stability[19] as well as interesting electro-optical properties[20]. Additionally, PANI is known to have comprehensive tunable properties originating from its structural flexibility which ultimately leads to many applications in the fields of anti-corrosive coatings, energy storage systems and gas sensing[21]. Conversely, copper oxide, a P-type semiconductor, is of particular interest in various applications including catalysis[22], semiconductors[23] gas sensors[24], biosensors[25], and field transistors[26] due to narrow band gap (1.2 eV), high specific surface area, good thermal conductivity, good electrochemical activity, antibiotic properties and photovoltaic properties[27]. The presence of CuO nanoparticles as impurities in carbon nanotubes based electrodes has been confirmed to be responsible for the electroxidation of glucose[28]. A glucose sensor fabricated by electrodepositing copper oxide nanocubes on graphene has shown good activity[29]. Furthermore, $CuO/Cu(OH)_2$ nanoparticles deposited on graphite-like carbon films exhib-

ited greater sensitivity and stability for sensing of glucose[30]. These studies suggest the importance of supporting material of CuO nanoparticles for its enhanced glucose sensing performance.

In the present work, PANI/CuO nanocomposites were prepared by in situ chemical polymerization of aniline and CuO nanoparticles and their activity was tested for non-enzymatic electrochemical glucose sensing. Various physicochemical and spectroscopic techniques were used to characterize the synthesized PANI/CuO nanocomposites. PANI/CuO nanocomposites were coated on copper substrate to make electrode for glucose detection. The results revealed that our synthesized PANI/CuO nanocomposites can be used as electrocatalysts for glucose detection and related applications.

2. Experimental

2.1 Reagents

All the reagents were of analytical grade and used without further purification except aniline which was distilled repeatedly for every experiment. Aniline, sodium hydroxide and ammonium persulphate were purchased from Merck (E. Merck, D-6100, Darmstadt, FR. Germany). Hydrochloric acid, copper acetate, acetic acid, and absolute ethanol were purchased from BDH London.

2.2 Synthesis of CuO nanoparticles

CuO nanoparticles were synthesized by wet chemical precipitation method. A 0.4 M solution of copper acetate was prepared, with 3 ml acetic acid added. Then the resulting solution was heated in boiling water bath for half an hour with constant stirring in a magnetic stirrer followed by the rapid addition of 30 ml concentrated solution of NaOH (6 m) to the boiling mixture. After the addition of NaOH, the blue solution immediately turned black. The solution was further stirred for 3 h, keeping the temperature at 100 °C. The final product was centrifuged and washed several times with deionized water and absolute ethanol, respectively. The black colored copper oxide nanoparticles were first dried in air for 18 h and then in an oven at 80 °C for 3 h and then stored in an air tight bottle.

2.3 Synthesis of PANI

Polyaniline was prepared via oxidative chemical polymerization method using hydrochloric acid as dopant and ammonium persulphate as oxidant. A 100 ml hydrochloric acid solution (0.2 m) was prepared, with 1.9 ml aniline monomer added and stirred at 0 °C in an ice bath for 10 minutes. Then a precooled ammonium persulphate solution (0.2 m) was added dropwise for half an hour with constant stirring at 0 °C. The solution was further stirred for 6 h in an ice bath by magnetic stirrer and then kept in a refrigerator for 18 h at 0 °C. The final product was filtered and washed with distilled water and ethanol respectively many times. After washing, the resultant polymer was dried in an oven at 80 °C for 6 h and stored in airtight bottle.

2.4 Synthesis of PANI/ CuO nanocomposites

Different percent composition of PANI/CuO nanocomposite were prepared by in situ chemical polymerization method using hydrochloric acid as dopant and ammonium persulphate as oxidant. A 100 ml hydrochloric acid solution (0.2 m) was taken to which aniline monomer was added and stirred at 0 °C for 10 minutes. Then a known weight of CuO nanoparticles was added to the aniline monomer solution and stirred for half an hour in an ice bath. Then 50 ml ammonium persulphate solution was added dropwise for 30 minutes keeping the temperature at 0 °C with constant stirring. The solution was further stirred at the same temperature for 6 h and then placed in a refrigerator for 18 h at 0 °C. The final product was washed with water and absolute ethanol respectively several times and then dried in an oven at 80 °C for 6 h. In this way, five different composites of PANI with 10%, 20%, 30% 40% and 50% (weight %) of CuO were prepared.

2.5 Fabrication of glucose sensor

PANI/CuO nanocomposites were coated on copper substrate. Prior to deposition, the substrate was cleaned with detergent, followed by ultrasonicationin distilled water, absolute ethanol and acetone for 20 minutes each, respectively. The substrates were then dried in an oven at 80 °C for 1 h.

The composites were deposited on copper by drop casting method. For this purpose, a small amount of the composite was dissolved in N-methylpyrrolidone and sonicated for 15 min. A few drops of the solution were drop casted onto the surface of copper that covered the surface completely. This step was followed by drying the electrode at 80 °C for 2 h and stored in air tight bottles before use.

2.6 Characterization

The surface morphology of PANI/CuO nanocomposites was characterized using scanning electron (JEOL, JAPAN, Model: JSM 5910). The XRD spectra were acquired by using XRD; JEOL-JDX: 3532) with Kα radiations (λ= 1.5406 Å). The spectra were obtained by scanning the samples from 5°−80° with a sampling pitch of 0.05° and step time of 1 s.The UV-Vis spectra were obtained from UV/Vis Perkin Elmer (spectrophotometer; UK), while FTIR was carried out using FTIR model Shimadzu, IR Prestige-21& FTIR 8400S. Cyclic voltammetry (CV) measurements were performed in an electrochemical cell consisting on working electrode, graphite counter electrode and (Ag/AgCl) as reference electrode coupled with a potentiostat (Gamry: USA, ZRA potentiostat ref 3000).

3. Results and discussion

3.1 XRD studies

Figure 1 (A) represents the XRD pattern of CuO nanoparticles. Well distinguished sharp peaks are observed at 2θ equal to 35° and 38°, while small peaks in the region 32°, 48°, 61° and 65°. All these XRD signals correspond to the CuO phase and consistent with the literature[31]. The average crystallite size of copper oxide nanoparticles was calculated by Debye-Scherrer equation:

$$D = K\lambda/\beta Cos\theta$$

Where, D is the average crystallite size, λ is the wavelength of X-rays, β is the full width half maximum of the peak and θ is the angular position of the peak. The average crystallite size was found to be equal to 49.19 nm. **Figure 1 (B)** represents the XRD pattern for synthesized PANI. The analysis of the XRD pattern reveals that there are no sharp peaks suggesting an amorphous phase for the prepared PANI. Furthermore, the XRD patterns of PANI/CuO nanocomposites, i.e., 10%, 20%, 30%,

40% and 50% shown in **Figure 1 (C-G)** suggest an amorphous phase for nanocomposites similar to that of the pure PANI.
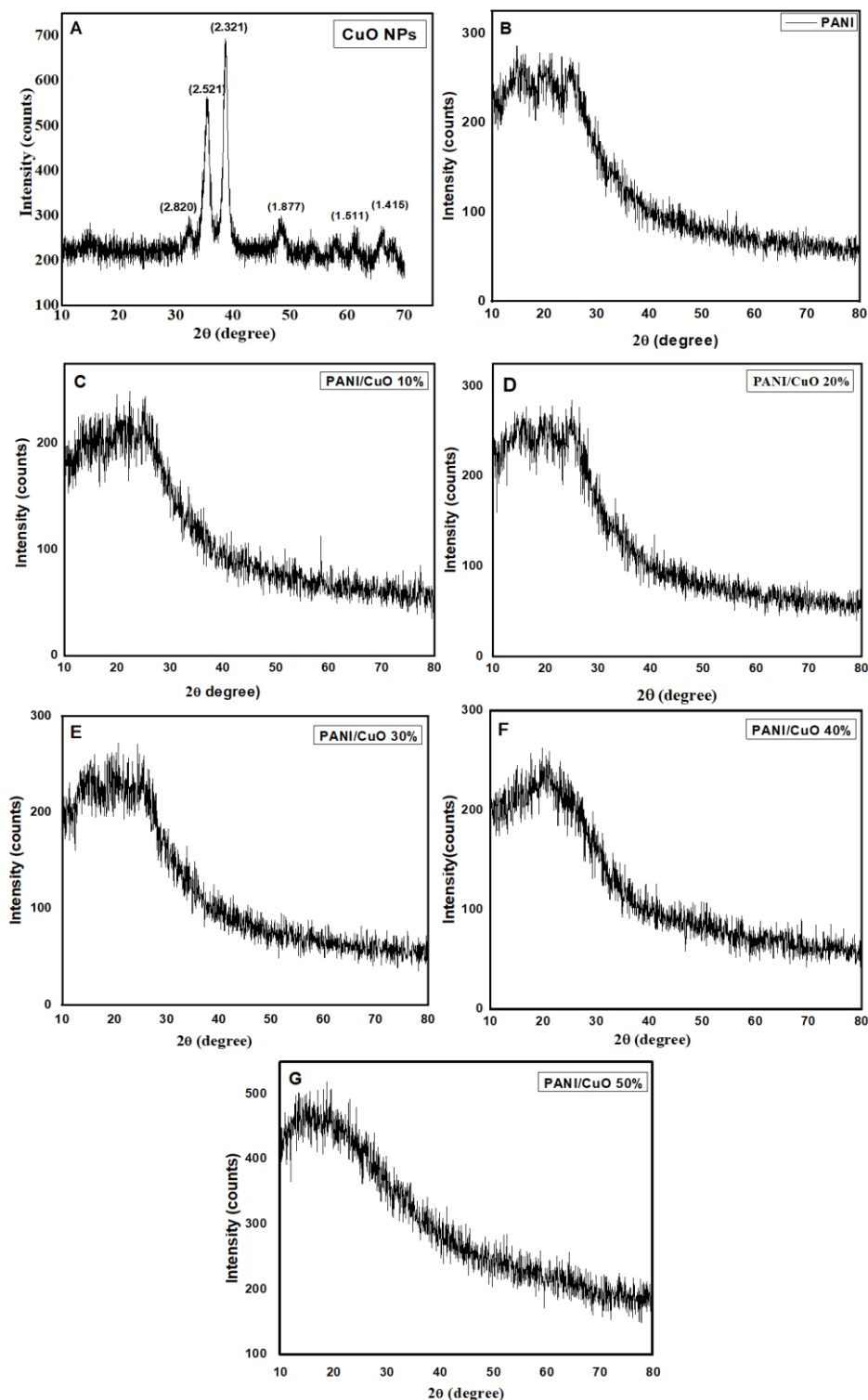

Figure 1. XRD patterns of (A) CuO nanoparticles, (B) PANI and different composition of PANI/CuO nanocomposite (C) 10% (D) 20% (E) 30% (F) 40% (G) 50%.

3.2 FTIR analysis

FTIR spectra of CuO nanoparticles are shown in **Figure 2 (A)**, the bands at 525 cm^{-1} to 750 cm^{-1} are assigned to the vibrations of the CuO functional group. The bands at the region 1404 cm^{-1} is due to the presence of carboxylate ions bound to CuO nanoparticles as bidentate ligand[32]. The band at 1639 cm^{-1} might be due to the formation of covalent bond between CuO nanoparticles and the –OH group

12

from adsorbed water.
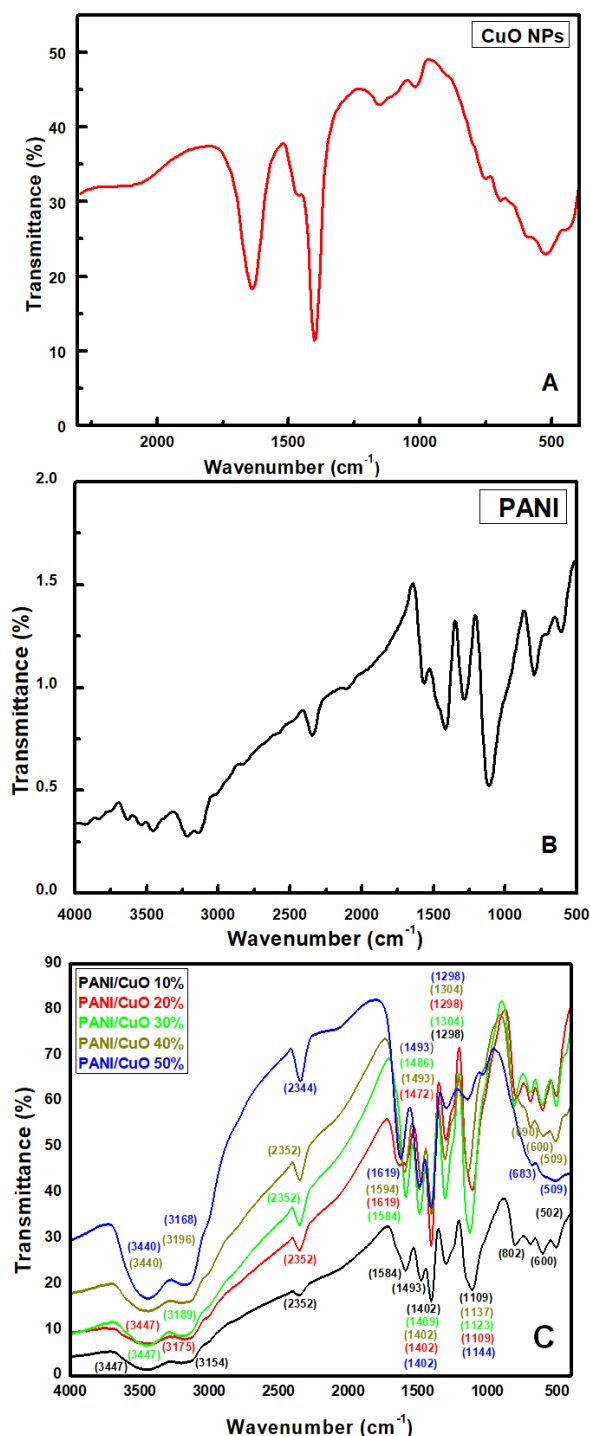
Figure 2. FTIR spectra of (A) CuO nanoparticles, (B) PANI, and(C) different percent composition of PANI/CuO nanocomposites.

The FTIR spectra of PANI and PANI/CuO nanocomposites are presented in **Figure 2 (B)** and **(C)**, respectively. The bands at 1569 cm^{-1} and 1426 cm^{-1} are assigned to the stretching mode of vibration of C = C and C = N of quinonoid and benzinoid units of PANI. The band at 1114 cm^{-1} is due to in plane bending vibrations of =C-H mode. The peak at 1283 cm^{-1} is assigned to C-N stretching vibration of benzenoid moiety of PANI. The peaks arise between values of 3216-3453 cm^{-1} is the result of N-H stretching vibration. The band at 788 cm^{-1} is due to out of plane bending vibration of =C-H. The FTIR spectra of nanocomposites are identical in shape with that of pure PANI with a slight red shift. The band at 1426 cm^{-1} is shifted to 1493 cm^{-1} in case of 10%, 40% and 50% nanocomposites, while the same band is shifted to 1486 cm^{-1} and 1472 cm^{-1} in case of 20% and 30% nanocomposites, respectively. The band at 1569 cm^{-1} is shifted to 1584, 1619, 1584, 1594 and 1619 cm^{-1} in case of 10, 20, 30, 40 and 50% nanocomposites, respectively. Moreover, there is band shifting from 1114 cm^{-1} to 1137, 1123, 1144, 1109 and 1109 cm^{-1} in case of 40, 20, 30, 10 and 50% nanocomposites, respectively. The band at 3216 cm^{-1} is shifted to lower wavenumber in all nanocomposites. All the above mentioned changes in the spectra reveal that there is some sort of interaction between PANI and CuO nanoparticles. This change has been attributed to the change in molecular order and slight loss of conjugation in PANI, resulting in strong localization of electrons over PANI ring[33].

3.3 UV-Vis spectroscopy

The UV-Vis spectra of CuO nanoparticles were obtained using water as solvent, while the UV-Vis spectra of PANI and all nano-composites were recorded using N-methylpyrrolidine as solvent. The UV-Vis spectra of CuO nanoparticles show a broad absorption peak at 290 nm, while that of PANI as shown in **Figure 3 (A)** has two distinctive broad bands at 330 nm and 641 nm. The spectra are identical to previous work in literature[34,35]. The band at 330 nm is attributed to π-π* transition of benzenoid ring, while the band at 640 nm is assigned to π-π* transition of quinoid ring of PANI.

The UV-Vis spectra of nanocomposites are shown in **Figure 3 (C)**. The general shape of the curve is similar to PANI and the shift in absorption band is obvious. The band at 330 nm in PANI is shifted to higher wavelengths in the composite material, i.e., from 330 nm to 326, 325, 320, 314 and 290 nm in 10, 20, 30, 40 and 50% nanocompo-

13

sites, respectively. The shift in the band at 642 nm is even much pronounced, i.e., from 642 nm to 639, 623, 622, 602 and 590 nm in 10, 20, 30, 40 and 50% nanocomposites, respectively.
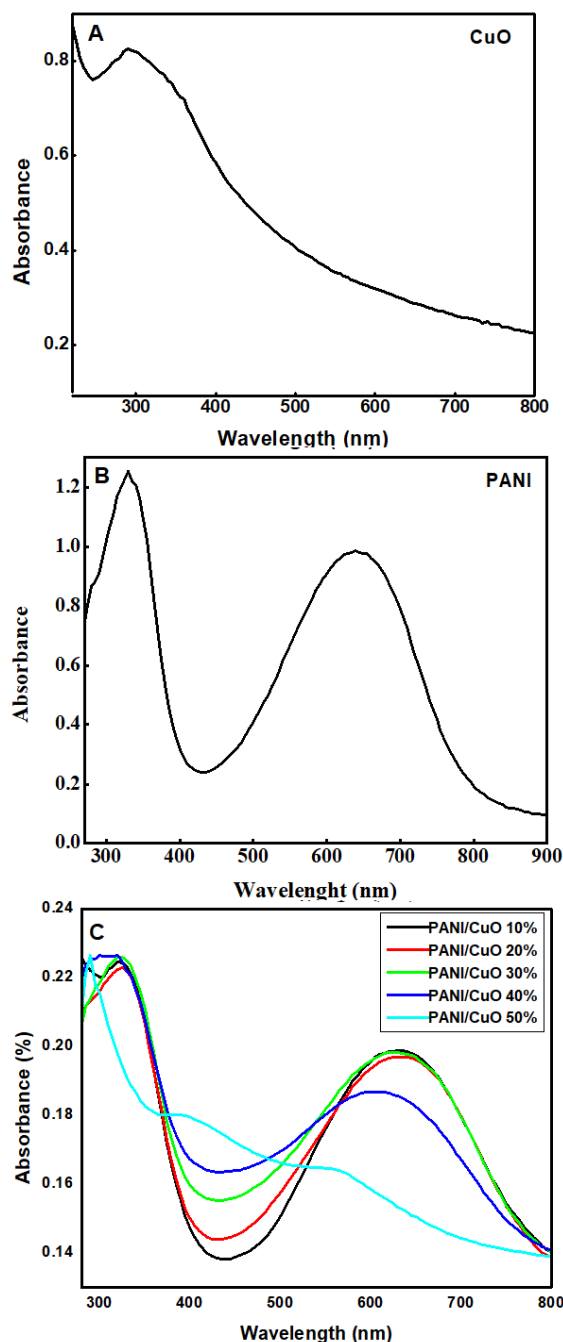

Figure 3. UV-Vis spectra of (A) Copper oxide, (B) PANI, and (C) different percent composition of PANI/CuO nanocomposites.

ticles was found to be 55.25 nm. As can be seen from the SEM image, the particles are fine, homogenous and granular. Surface morphology of the prepared PANI is shown in **Figure 4 (B)** which shows that PANI has a highly porous structure. One can easily conclude from the image that it has a high surface area. Moreover, fussy surface morphology with interconnected fibers can also be seen from the image. The SEM images of the nanocomposites shown in **Figure 4 (C-G)** reveal that the incorporation of nanoparticles into PANI has a significant effect on its morphology.
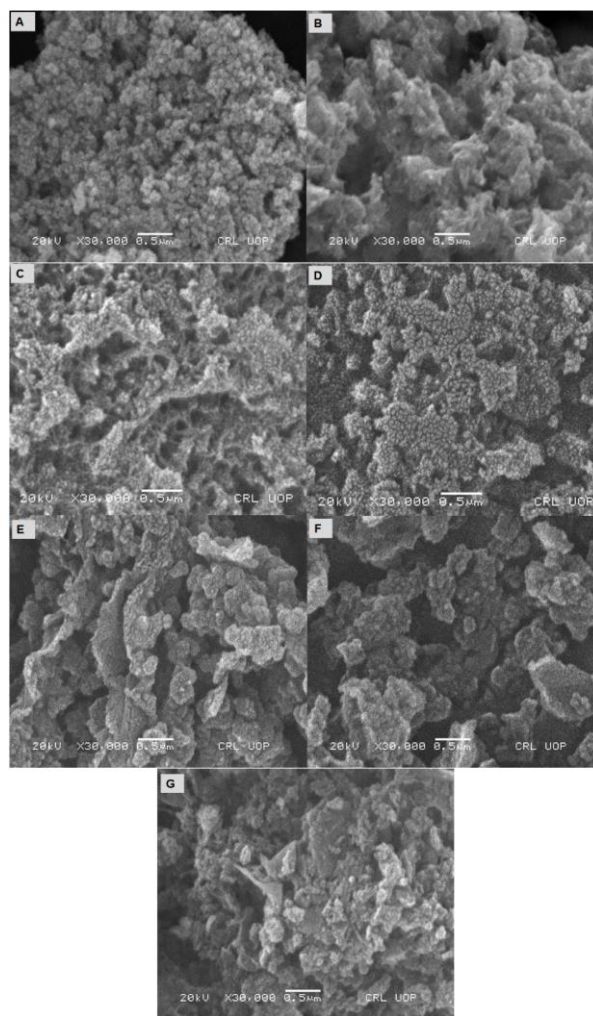

Figure 4. SEM images of **(A)** copper oxide nanoparticles, **(B)** PANI, and **(C-G)** different percent composition of PANI /CuO nanocomposites with 10%, 20%, 30%, 40% and 50% CuO, respectively.

3.4 Morphology of PANI/CuO

Figure 4 (A) shows the SEM image of pure CuO nanoparticles. From the image, we can see the surface morphology of the finely dispersed nanoparticles.

The average particle size of the CuO nanopar-

From the **Figure 4 (C)** PANI/CuO 10%, it can be seen that the finely dispersed nanoparticles are loaded into PANI fibers, resulting a decrease in porosity. The image also suggests that there are no bare or free nanoparticles and all the nanoparticles are incorporated by the polymer uniformly.

14

Thus, it can be concluded that this method can be used to prepare uniformly dispersed layer of nano-particles. The SEM image of PANI/CuO 20% in **Figure 4** (D) shows that the increase in weight of nanoparticles has further decreased the porosity and the particles are now more tightly packed. Further-more, the SEM images of composites with percent composition of 30, 40 and 50% shown in **Figure 4 (E-G)** are further closely packed as compared with 20% loading of nanoparticles. The nanoparticles have been homogenously incorporated into the polymer matrix.

3.5 Electrochemical glucose sensing

Figure 5 represents the cyclic voltammetry of PANI/CuO (10%) in the absence and presence of glucose in 0.1 M NaOH solution. In the absence of glucose, there is no distinguished peak as can be seen in the figure. When glucose is added into solu-tion, there is a well distinguished peak around 0.65 V corresponding to irreversible oxidation of glucose. Further, the current density of the peak is propor-tional to the concentration of glucose in solution during cyclic voltammetry. The peak current im-proved over the potential range of 0.4 to 0.65 V following addition of 4-10 mM of glucose.

13
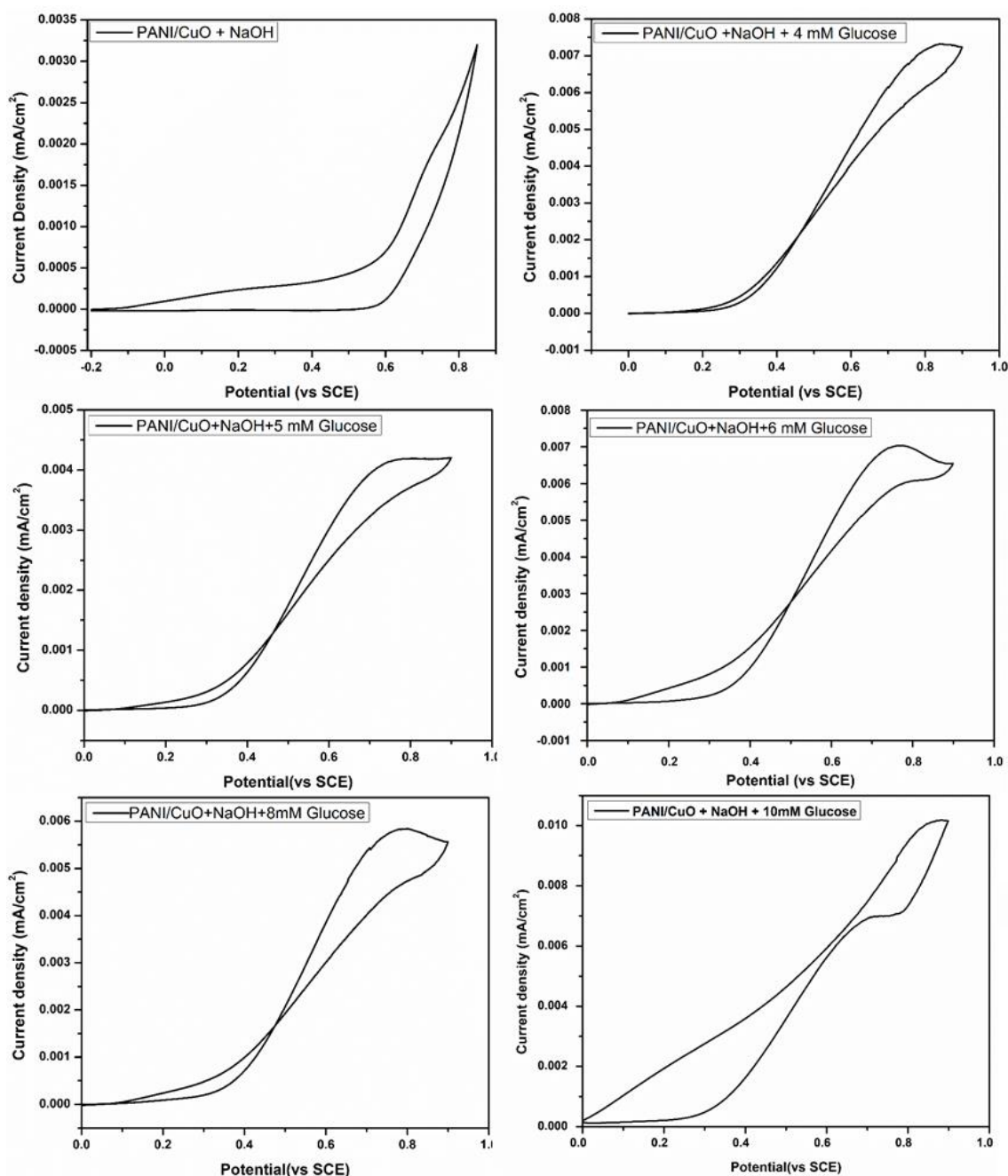
Figure 5. Cyclic voltammograms of PANI/CuO (10%) in NaOH solution in the absence and presence of various glucose concentrations.

4. Conclusion

In summary, PANI/CuO nanocomposites have been successfully synthesized by in situ chemical polymerization of aniline and CuO nanoparticles. The synthesized samples were characterized by various techniques, including XRD, SEM, UV-Vis spectroscopy, FTIR, and cyclic voltammetry. With the addition of CuO nanoparticles into the matrix of PANI, the crystallinity remained unchanged while the UV-Vis absorption properties altered drastically. In addition, the surface morphology varied with CuO composition in the composites. When tested for electrochemical detection of glucose, the PANI/CuO (10 %) electrode exhibited good response, thus indicating its potential as electrocatalyst for electrochemical glucose sensing applications.

Acknowledgement

References

1. Wang G, He X, Wang L, *et al*. Non-enzymatic electrochemical sensing of glucose. Microchimica Acta 2013; 180(3-4): 161–186.
2. Newman JD, Turner AP. Home blood glucose biosensors: A commercial perspective. Biosensors & Bioelectronics 2005; 20(12): 2435–2453.
3. Deng C, Chen J, Chen X, *et al*. Direct electrochemistry of glucose oxidase and biosensing for glucose based on boron-doped carbon nanotubes modified electrode. Biosensors & Bioelectronics 2008; 23(8): 1272–1277.
4. Wilson R, Turner APF. Glucose oxidase: an ideal enzyme. Biosensors & Bioelectronics 1992; 7(3): 165–185.
5. Kang X, Mai Z, Zou X, *et al*. A novel glucose biosensor based on immobilization of glucose oxidase in chitosan on a glassy carbon electrode modified with gold–platinum alloy nanoparticles/multiwall carbon nanotubes. Analytical biochemistry 2007; 369(1):71–79.
6. Li L, Zhang W. Preparation of carbon nanotubes supported platinum nanoparticles by an organic colloidal process for nonenzymatic glucose sensing. Microchimica Acta 2008; 163(3-4): 305–311.
7. Li Y, Song Y, Yang C, *et al*. Hydrogen bubble dynamic template synthesis of porous gold for nonenzymatic electrochemical detection of glucose. Electrochemistry Communications 2007; 9(5): 981–988.
8. Wang J, Thomas DF, Chen A. Nonenzymatic electrochemical glucose sensor based on nanoporous PtPb networks. Analytical Chemistry 2008; 80(4): 997–1004.
9. Chen X, Pan H, Liu H, *et al*. Nonenzymatic glucose sensor based on flower-shaped Au@ Pd core–shell nanoparticles–ionic liquids composite film modified glassy carbon electrodes. Electrochimica Acta 2010; 56(2): 636–643.
10. Sattar M, Conway B. Electrochemistry of the nickel-oxide electrode—VI. Surface oxidation of nickel anodes in alkaline solution. Electrochimica Acta 1969; 14(8): 695–710.
11. Wang J, Zhang W. Fabrication of CuO nanoplatelets for highly sensitive enzyme-free determination of glucose. Electrochimica Acta 2011; 56(22): 7510–7516.
12. Chowdhury AD, Gangopadhyay R, De A. Highly sensitive electrochemical biosensor for glucose, DNA and protein using gold-polyaniline nanocomposites as a common matrix. Sensors and Actuators B: Chemical 2014; 190: 348–356.
13. Yavuz AG, Uygun A, Bhethanabotla VR. Preparation of substituted polyaniline/chitosan composites by in situ electropolymerization and their application to glucose sensing. Carbohydrate Polymers 2010; 81(3): 712–719.
14. Luo J, Jiang S, Zhang H, *et al*. A novel non-enzymatic glucose sensor based on Cu nanoparticle modified graphene sheets electrode. Analytica Chimica Acta 2012; 709: 47–53.
15. Adeloju S, Wallace G. Conducting polymers and the bioanalytical sciences: new tools for biomolecular communications. A review. Analyst 1996; 121(6): 699–703.
16. Kang Y, Kim SK, Lee C. Doping of polyaniline by thermal acid–base exchange reaction. Materials Science and Engineering: C 2004; 24(1-2): 39–41.
17. Pruneanu S, Veress E, Marian I, *et al*. Characterization of polyaniline by cyclic voltammetry and UV-Vis absorption spectroscopy. Journal of Materials Science 1999; 34(11): 2733–2739.
18. Wang X, Geng Y, Wang L, *et al*. Thermal behaviors of doped polyaniline. Synthetic Metals 1995; 69(1-3): 265–266.
19. Chiang JC, MacDiarmid AG. 'Polyaniline': protonic acid doping of the emeraldine form to the metallic regime. Synthetic Metals 1986; 13(1-3): 193–205.
20. Malile B. Exploring the potential of polyelectrolyte-aptamer films for use in optical and electrochemical sensing [Master's thesis]. York University: York University; 2015. p. 72.
21. Dhand C, Das M, Datta M, *et al*. Recent advances in polyaniline based biosensors. Biosensors & Bio-

electronics 2011; 26(6): 2811–2821.

22. Chen J, Deng S, Xu N, *et al*. Temperature dependence of field emission from cupric oxide nanobelt films. Applied Physics Letters 2003; 83(4): 746–748.

23. Meyer B, Polity A, Reppin D, *et al*. Binary copper oxide semiconductors: From materials towards devices. Physica Status Solidi B 2012; 249(8): 1487–1509.

24. Chowdhuri A, Gupta V, Sreenivas K, *et al*. Response speed of SnO_2-based H_2S gas sensors with CuO nanoparticles. Applied Physics Letters 2004; 84(7): 1180–1182.

25. Luque GL, Rodríguez MC, Rivas GA. Glucose biosensors based on the immobilization of copper oxide and glucose oxidase within a carbon paste matrix. Talanta 2005; 66(2): 467–471.

26. Zheng X, Xu C, Tomokiyo Y, *et al*. Observation of charge stripes in cupric oxide. Physical Review Letters 2000; 85(24): 5170–3.

27. Rai V, Jamuna B. Science against microbial pathogens: Communicating current research and technological advances. In: Mendez-Vilas A(editor). Karnataka, India: University of Mysore; 2011. p. 197.

28. Batchelor-McAuley C, Wildgoose GG, Compton RG, *et al*. Copper oxide nanoparticle impurities are responsible for the electroanalytical detection of glucose seen using multiwalled carbon nanotubes. Sensors and Actuators B: Chemical 2008; 132(1): 356–360.

29. Luo L, Zhu L, Wang Z. Nonenzymatic amperometric determination of glucose by CuO nanocubes–graphene nanocomposite modified electrode. Bioelectrochemistry 2012; 88: 156–163.

30. You T, Niwa O, Tomita M, *et al*. Characterization and electrochemical properties of highly dispersed copper oxide/hydroxide nanoparticles in graphite-like carbon films prepared by RF sputtering method. Electrochemistry Communications 2002; 4(5): 468–471.

31. Manjunath A, Irfan M, Anushree KP, *et al*. Synthesis and Characterization of CuO Nanoparticles and CuO Doped PVA Nanocomposites. Advances in Materials Physics and Chemistry 2016; 6(10): 263.

32. Taman R, Salem M, Ossman M, *et al*. Metal oxide nano-particles as an adsorbent for removal of heavy metals. Journal of Advanced Chemical Engineering 2015; 5(3): 1–8.

33. Jundale D, Navale ST, Khuspe GD, *et al*. Polyaniline–CuO hybrid nanocomposites: synthesis, structural, morphological, optical and electrical transport studies. Journal of Materials Science: Materials in Electronics 2013; 24(9): 3526–3535.

34. Kumar A, Kumar D, Pandey G. Characterisation of hydrothermally synthesised CuO nanoparticles at different pH. Journal of Technological Advances and Scientific Research 2016; 2(4): 166–169.

35. Godovsky DY, Varfolomeev AE, Zaretsky DF, *et al*. Preparation of nanocomposites of polyaniline and inorganic semiconductors. Journal of Materials Chemistry 2001; 11(10): 2465–2469.